

# The effect of adding a bit of Fe to Ag-Ge-Se system

Bibiana Arcondo<sup>1</sup>, María Andrea Ureña<sup>1,2</sup>, Maximiliano Erazú<sup>1</sup>, Javier Rocca<sup>1</sup>,  
Marcelo Fontana<sup>1,2</sup>

1. *INTECIN, Facultad de Ingeniería, Universidad de Buenos Aires-CONICET*

2. *C.I.C, CONICET*

## ***Abstract.***

Ag-Ge-Se system is an easy glass former in a wide composition range not far from the Se corner of the equilibrium phase diagram. The existence of a liquid miscibility gap impacts on the glass morphology where Ag-rich zones alternate with Ag depleted ones which size depends on composition. In order to analyze the short range order, 0.5 at. % Fe was added as a probe in the synthesis stage.

Mössbauer spectra of these glasses were obtained at room and lower temperatures. Two types of environments were observed. The corresponding Debye temperatures, and the fraction of Fe atoms in each environment were determined.

Additionally, magnetic moment was measured as a function of temperature and applied magnetic field. From  $m(H)$  and  $m(T)$  curves it is evident that the magnetization of the glasses has two components, i.e., a blocked one even up to room temperature that saturates at low field, and a paramagnetic one which does not saturate even at the largest applied field.

The Mössbauer spectroscopy results are discussed and correlated to the morphology and magnetic behavior of these glasses.

*Keywords: Chalcogenide glasses, Mössbauer effect, Magnetic properties*

## ***1. Introduction.***

### **1.1 Ge-Se SYSTEM**

$\text{Ge}_x\text{Se}_{1-x}$  system is an easy glass former for  $x \leq 0.43$  atomic fraction. The glasses are covalently bonded and the connectivity and other properties of the network are strongly dependent on composition. This network structure presents the so called intermediate range order (IRO) which manifestation is a first sharp diffraction peak (FSDP) of the total structure factor  $S(q)$ , observed at  $q \approx 1 \text{ \AA}^{-1}$ .

The structure of these network glasses has been widely investigated either by means of X-rays and neutron diffraction [1 and references therein] or employing a complete gamma of techniques (i.e.  $^{119}\text{Sn}$  and  $^{129}\text{I}$  Mössbauer spectroscopy [2]).

Boolchand and collaborators [3, 4] point out that two structural transitions take place in this system:  $\text{Ge}_x\text{Se}_{1-x}$  glasses are described as floppy for  $x \leq 0.20$  and rigid for  $x \geq 0.26$  whereas an intermediate phase is proposed in between. From modulated differential calorimetry experiments these authors conclude that the intermediate phase network is stress free as the irreversible component of enthalpy is meaningless. The structure of Se rich glasses consists of Se chains linked by Ge atoms tetrahedrally coordinated by Se.

As the composition approximates that of  $\text{GeSe}_2$ , the structure consists of chains of corner or edge sharing  $\text{GeSe}_{4/2}$  tetrahedra. [5, 6]

However homopolar bonds are found to be a characteristic feature of  $\text{GeSe}_2$  glasses [1] and Ge-Ge bonds are the main contribution to the FSDP of the total structure factor measured.

When Ag is added to  $\text{Ge}_x\text{Se}_{1-x}$  in the intermediate phase composition range the glass forming tendency is not substantially affected whereas it impacts notably on the transport properties. [7, 8, 9]

## 1.2 Ag-Ge-Se SYSTEM

The equilibrium phase diagram of the Ag-Ge-Se system was compiled and evaluated by Prince. [10]

Ag<sub>2</sub>Se-GeSe<sub>2</sub> pseudo binary system allows the invariant equilibria in the ternary system to be considered as two partial ternary systems: Ag<sub>2</sub>Se-GeSe<sub>2</sub>-Se [Figure 1] and Ag<sub>2</sub>Se-GeSe<sub>2</sub>-Ge-Ag. Ag<sub>8</sub>GeSe<sub>6</sub>, which melts congruently at 902°C, separates two eutectics on the pseudo binary Ag<sub>2</sub>Se-GeSe<sub>2</sub>: e<sub>1</sub> occurs at 560°C and e<sub>2</sub> occurs at 810°C.

The pseudo binary section Ag<sub>8</sub>GeSe<sub>6</sub>-Se divides the partial ternary system Ag<sub>2</sub>Se-GeSe<sub>2</sub>-Se.

A monotectic reaction,  $L_1 \leftrightarrow Ag_8GeSe_6 + L_2$ , occurs at 700°C. This reaction falls in temperature within the ternary and closes up the region of liquid immiscibility at a critical tie line  $L_1/L_2 \leftrightarrow Ag_8GeSe_6$  at 520°C.

The eutectic separation of Ag<sub>8</sub>GeSe<sub>6</sub> + GeSe<sub>2</sub> is shown by a monovariant curve descending from the eutectic e<sub>1</sub> towards the Se corner. In the projection of the liquidus, this curve intersects the liquid miscibility gap at L<sub>7</sub>, showing the presence of a ternary monotectic reaction,  $L_7 \leftrightarrow L_8 + Ag_8GeSe_6, GeSe_2$  at 400°C.

The solidification in the Ag<sub>8</sub>GeSe<sub>6</sub>-GeSe<sub>2</sub>-Se system ends with an eutectic reaction in the Se rich corner at 217°C.

The interest on this ternary system is due to fundamental aspects (i.e. large glass forming composition range that let us to analyze the dependence of glass properties on composition or structure) as well as actual or potential applications (i.e. solid state

electrolyte; optochemical/electrochemical sensors; switching devices; storage elements, etc.).

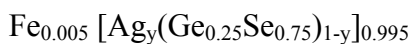
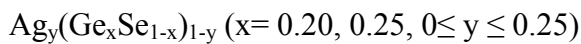
To collaborate to structural analyses of this system, a small amount of Fe was incorporated in the synthesis stage of the samples as a Mössbauer probe and then the magnetic properties of the new system were analyzed.

## ***2. Experimental procedure***

The components in the desired stoichiometry were arranged in 10 mm diameter quartz tubes evacuated to  $3 \cdot 10^{-5}$  mbar and sealed. The batches were heated in a furnace at 910°C for 8 hrs and then, either quenched in a mixture of ice-water or slowly cooled. The element purity is 99.99% for Ge, Se and 99.9% for Ag.

0.5% Fe (>90%  $^{57}\text{Fe}$ ) was added to the samples stoichiometry in the synthesis step.

*Sample compositions:*



Scanning electron microscopy measurements were carried out employing an acceleration voltage of 25 kV in a Philips XL 30CP equipment. The structure was characterized by means of X-Ray diffractometry employing  $\text{Cu K}_\alpha$  radiation.

Mössbauer measurements were performed at different temperatures, in transmission geometry, employing a  $^{57}\text{Co}(\text{Rh})$  source. The spectra were fitted employing sites or quadrupole splitting ( $\Delta$ ) distributions with the Normos programs (Dist and Site) [11].

Isomer Shift ( $\delta$ ) is reported relative to  $\alpha\text{-Fe}$ .

Additionally, magnetic moment was measured on samples containing Fe as a function of temperature and applied magnetic field in a Quantum Design PPMS magnetometer.

ZFC and FC moment density as a function of T was measured after application of a 500Oe magnetic field, AC magnetization was measured under a 10Oe field ( $f=1\text{Mhz}$ ).

### ***3. Previous results***

The existence of intermediate range order (**IRO**) associated to a prepeak or first sharp diffraction peak (**FSDP**), around  $1.0 \text{ \AA}^{-1}$ , in the structure factor  $S(q)$  of  $\text{Ag}_y(\text{Ge}_{0.25}\text{Se}_{0.75})_{1-y}$  samples has been observed. [12] The **FSDP** position of the ternary glasses is slightly moved with respect to that of the binary glass. The **FSDP** area decreases due to a change of the **IRO** upon adding Ag.

Electric conductivity measurements performed on bulk samples using the impedance spectroscopy technique in the frequency range from 5 Hz to 2 MHz, at temperatures from 293K to 363K, show an abrupt jump in conductivity with  $0.07 < y < 0.08$  corresponding to a change of conductivity regime from semiconductor to fast ionic conductor. [8, 9]

## 4. Results and discussion

### *Ag<sub>y</sub>(Ge<sub>x</sub>Se<sub>1-x</sub>)<sub>1-y</sub> glasses*

Morphology of bulk glasses with  $y=0.07$  (A, B) and  $y=0.20$  (C, D) are shown in Figure 2. Bright zones (Ag rich) immersed in a dark matrix (Ag depleted) are observed in samples with  $y=0.07$  whereas dark zones immersed in a bright matrix are observed in samples with  $y=0.20$ .

The average diameter of the nearly circular zones are 110nm for  $\text{Ag}_{0.07}(\text{Ge}_{0.25}\text{Se}_{0.75})_{0.93}$  (A) and 160nm for  $\text{Ag}_{0.07}(\text{Ge}_{0.20}\text{Se}_{0.80})_{0.93}$  (B) and about  $0.7\mu\text{m}$  for  $\text{Ag}_{0.20}(\text{Ge}_{0.25}\text{Se}_{0.75})_{0.80}$  (C) and  $2\mu\text{m}$  for  $\text{Ag}_{0.20}(\text{Ge}_{0.20}\text{Se}_{0.80})_{0.80}$  (D).

Accordingly, a main tendency shall be remarked: the scale of the inhomogeneities grows (from nm to  $\mu\text{m}$ ) as the composition approaches the composition of the miscibility gap in the ternary phase diagram.

Half way between samples with low and high Ag content is a sample which composition is  $\text{Ag}_{0.08}(\text{Ge}_{0.25}\text{Se}_{0.75})_{0.92}$ . This sample corresponds to the semiconducting to ionic conductivity transition and shows that this phenomenon is associated to a percolation transition having place for a volume fraction of the bright phase nearby the well known Scher –Zallen threshold (15% ). [13, 14] The highest Ag concentration sample analyzed, which composition is  $\text{Ag}_{0.25}(\text{Ge}_{0.25}\text{Se}_{0.75})_{0.75}$ , is a fast ionic conductor and, as well as the others, intrinsically non homogeneous. Nevertheless, its microstructure does not resemble that of samples with lower Ag concentration.

Other chalcogenide glasses have similar behavior: non homogeneous glasses that present abrupt transition from semiconductor to fast ionic conductor have been reported by Pradel and collaborators in [15].

*Fe<sub>0.005</sub> [Ag<sub>y</sub> (Ge<sub>0.25</sub>Se<sub>0.75</sub>)<sub>1-y</sub>]<sub>0.995</sub> glasses*

Fe addition does not impact neither on the glass structure nor on its microstructure. Amorphous samples containing 0.5% Fe do not present apparent Fe segregation. However, small precipitates of a second phase, spread in the Ag<sub>2</sub>Se matrix, were observed when 0.5% Fe was added to Ag<sub>2</sub>Se (slowly cooled sample). These precipitates are not observed for samples quenched in air.

Mössbauer spectra of Fe<sub>0.005</sub> [Ag<sub>y</sub> (Ge<sub>0.25</sub>Se<sub>0.75</sub>)<sub>1-y</sub>]<sub>0.995</sub> glasses were fitted with two  $\Delta$  distributions corresponding to two different Fe environments. A distribution characterized by a large  $\Delta$  doublet (with peak values  $\delta=0.70\text{mm/s}$ ,  $\Delta=2.86\text{mm/s}$  at room temperature) corresponds to high spin (HS) Fe<sup>2+</sup> in distorted octahedral environments and the other characterized by a relatively small  $\Delta$  corresponds to low spin (LS) Fe<sup>2+</sup> in octahedral coordination (with peak values  $\delta=0.29\text{mm/s}$ ,  $\Delta=0.24\text{mm/s}$  at room temperature). As Ag concentration increases the larger  $\langle \Delta \rangle$  interaction grows as can be seen in Figure 3.

With the aim to determine the Debye temperature ( $\theta_D$ ) corresponding to each Fe environment, Mössbauer spectra were obtained at different temperatures (Figure 4): room temperature, 195K (in a mixture of dry ice and acetone) and 77K (in liquid nitrogen). From the Debye model dependence of the recoilless fraction  $f$  on temperature (T)

$$f = e^{-\frac{3E_\gamma^2}{4k_B\theta_D Mc^2}} \times \left\{ 1 + 4 \left( \frac{T}{\theta_D} \right)^2 \int_0^{\theta_D/T} \frac{x dx}{e^x - 1} \right\}$$

where  $E_\gamma = 14.4$  keV,  $M$  the atomic mass of  $^{57}\text{Fe}$ ,  $k_B$  the Boltzmann constant,  $c$  the speed of light and  $\theta_D$  the Debye temperature, under the supposition that the relative abundance of HS and LS  $\text{Fe}^{2+}$  sites remains constant, one can write for each environment

$$\ln\left(\frac{f}{f_0}\right) = \ln\left(\frac{A}{A_0}\right) = -\frac{3E_\gamma^2}{Mc^2k_B\theta_D} \times \left[ \frac{T^2}{\theta_D^2} \int_0^{\theta_D/T} \frac{x}{e^x - 1} dx - \frac{T_0^2}{\theta_D^2} \int_0^{\theta_D/T_0} \frac{x}{e^x - 1} dx \right]$$

where  $A$  is the integrated area of each contribution at  $T$  and  $A_0$  the corresponding area at  $T_0$ , with  $T_0 = \text{Room Temperature}$ .

As  $T \leq \theta_D$ ,  $I(\theta_D/T) = \int_0^{\theta_D/T} \frac{x}{e^x - 1} dx$  does not depend strongly on  $T$ . Therefore  $I(\theta_D/T)$

can be replaced by its average value in the range  $T < \theta_D$ .

A linear dependence of  $\ln(A/A_0)$  on  $T^2$  is verified and, from the corresponding slope,  $m$ ,  $\theta_D$  is determined for HS and LS sites as

$$\theta_D = \left( \frac{3E_\gamma^2}{Mc^2k_B m} \times \overline{I(\theta_D/T)} \right)^{1/3}$$

$\theta_D = 290\text{K}$  for HS  $\text{Fe}^{2+}$  and  $\theta_D = 370\text{K}$  for LS  $\text{Fe}^{2+}$  for samples with  $y = 0.10$

As Ag concentration increases the lower  $\theta_D$  regions grow in correspondence to the increase of the bright zones area in SEM images whereas Ag depleted zones with a persistent IRO correspond to higher  $\theta_D$ .

Nevertheless, for sample with  $x = 0.25$  which microstructure is singular,  $\theta_D = 316\text{K}$  for HS  $\text{Fe}^{2+}$  and  $\theta_D = 270\text{K}$  for LS  $\text{Fe}^{2+}$ . However as LS  $\text{Fe}^{2+}$  area decreases more than

that of HS  $\text{Fe}^{2+}$  as T increases, a spin switch from LS to HS states cannot be discarded and, in that case,  $\theta_D$  estimation should be corrected accordingly.

Once determined  $\theta_D$  for each environment, the corresponding  $f$  can be estimated and also the fraction of Fe atoms in each type of environment.  $26 \pm 3\%$  of Fe atoms in samples with a Ag content  $y=0.10$ , are in LS environments whereas  $74 \pm 3\%$  of Fe atoms are in HS environments.

Figure 5 shows the temperature dependence of the magnetic moment density  $\sigma(T)$  and the in phase component of magnetic moment density  $\sigma'_{ac}(T)$ . A Curie type curve ending in a plateau is observed in  $\sigma'_{ac}(T)$ . Figure 6 shows the field dependence of the magnetic moment density  $\sigma(H)$  of sample with  $y=0.10$  at 5K, 15K and 100K.

From  $\sigma(H)$  and  $\sigma(T)$  curves it is evident that the magnetization of the glasses has two contributions, a blocked one even up to room temperature that saturates at low field and a paramagnetic one which relative weight decreases as T grows and does not saturate even at the largest applied field. The fitting of the  $\sigma(H)$  curves considering a hysteretic curve plus a Brillouin function is also shown. The saturation value of both contributions has been estimated. It is observed that the saturation value of the paramagnetic contribution increases with Ag concentration.

As a consequence, the paramagnetic contribution is attributed to the Ag rich phase, that is, to HS  $\text{Fe}^{2+}$  environment that involves 26% Fe atoms and the smaller  $f$  value (0.61 for sample with  $y=0.10$  at 100K). Accordingly, the effective magnetic moment per Fe atom is, at 100K,  $m_{\text{HS}}=0.46\mu_B$ . On the other hand, the blocked contribution is attributed to the Ag depleted zones, that is, to the LS  $\text{Fe}^{2+}$  environments that involves 74% Fe atoms and the larger  $f$  values (0.74 for sample with  $y=0.10$  at 100K). The resulting effective magnetic moment per Fe atom is, at 100K,  $m_{\text{LS}}=0.0074\mu_B$ .

## 5. Conclusions

$\text{Ag}_y(\text{Ge}_x\text{Se}_{1-x})_{1-y}$  glasses with Ge atomic fractions  $x=0.20$  and  $0.25$  and  $0 \leq y \leq 0.25$  at fraction, obtained by melt quenching, present intrinsic inhomogeneity consisting of zones of different composition, basically due to Ag concentration.

The inhomogeneity size can be controlled with the overall composition and a small addition of Fe does not impact in these general trends.

A percolation transition occurs for a Ag composition below 10 at.%. For samples with  $x=0.25$  the percolation threshold corresponds to  $y \sim 0.08$ . As a consequence of the percolation of Ag rich zones a ionic conducting network connects the entire sample and a change in the electric transport behavior takes place.

Mössbauer analyses on samples with 0.5 at.% Fe let us see that the increasing of Ag concentration as well as increases the volume of Ag rich zones changes the bonding characteristics of both of the phases involved. That is, as Ag concentration changes, also does the Debye temperature of both phases. However, a spin switch cannot be discarded in sample with  $y=0.25$ .

Magnetic results show that  $\text{Fe}_{0.005}[\text{Ag}_y(\text{Ge}_{0.25}\text{Se}_{0.75})_{1-y}]_{0.995}$  glasses can be modeled as a superposition of a paramagnetic component involving HS  $\text{Fe}^{2+}$  atoms plus other characterized by a small remanence and hysteretic fields below 300Oe involving LS  $\text{Fe}^{2+}$  atoms with no correlation with any hyperfine field in Mössbauer spectra. This fact can be attributed either to the different conditions of both experiments (i.e. external field) or to the small magnetic moment per atom involved in the blocked component.

## ***Acknowledgements***

The authors are grateful to:

*ANPCyT (project PICT03-14383) and Universidad de Buenos Aires (project IN023)* for their support.

*Dr. M.F. Van Raap* for her friendly collaboration with low temperature Mössbauer measurements.

*Technological Research Centre(CINI) Tenaris S.A., Argentina,* for Scanning Electron Microscopy.

*Argentine Network of Magnetism and Magnetic Materials, RN3M,* as magnetic measurements were performed with the network equipment.

## ***References***

1. Salmon, P.S.: Structure of liquids and glasses in the Ge-Se binary system, J. Non-Cryst.Solids 353, 2959 (2007).
2. Boolchand, P. and Bresser, W.J.: The structural origin of broken chemical order in GeSe<sub>2</sub> glass, Phil. Mag. B, 80, 1757 (2000).
3. Boolchand, P. Feng, X. and Bresser, W.J.: Rigidity transitions in binary Ge–Se glasses and the intermediate phase, J. Non-Cryst Solids 293-295, 348 (2001).
4. Boolchand, P. Georgiev, D.G. Qu, T. Wang, F. Cai, L. Chakravarty, S.: Nanoscale phase separation effects near  $\bar{r} = 2.4$  and 2.67, and rigidity transitions in chalcogenide glasses C.R. Chimie 5, 713 (2002).

5. N. Ramesh Rao, P.S.R. Krishna, S.Basu, B.A. Dasannacharya, K.S. Sangunni and E.S.R. Gopal: Structural correlations in  $\text{Ge}_x\text{Se}_{1-x}$  glasses – a neutron diffraction study, *J.Non-Cryst. Solids* 240, 221 (1998).
6. P.Armand, A.Ibanez, H.Dexpert, D.Bittencourt, D.Raoux and E.Philippot: Structural approach of Ge-X,  $\text{GeX}_2\text{-Ag}_2\text{X}$  (X=S,Se) glassy systems, *J. de Physique IV Colloque C2 2*, C2-189 (1992).
7. M. Kawasaki, J. Kawamura, Y. Nakamura, M. Aniya: Ionic conductivity of  $\text{Ag}_x(\text{GeSe}_3)_{1-x}$  ( $0 \leq x \leq 0.571$ ) glasses, *Solid State Ionics* 123, 259 (1999).
8. M.A. Ureña, A.A. Piarristeguy, M. Fontana and B. Arcondo: Ionic conductivity ( $\text{Ag}^+$ ) in  $\text{AgGeSe}$  glasses., *Solid State Ionics* 176, 505 (2005).
9. A. Piarristeguy, J.M. Conde Garrido, M.A. Ureña, M. Fontana, B. Arcondo: Conductivity percolation transition of  $\text{Ag}_x(\text{Ge}_{0.25}\text{Se}_{0.75})_{100-x}$  glasses, *Journal of Non-Crystalline Solids* 353, 3314 (2007).
10. A. Prince, in: Ternary Alloys, ed. G. Petzow and G. Effenberg (VCH. New York. 1988) p. 195.
11. Brand, R.A. NORMOS Programs, 1990.
12. A. Piarristeguy, M. Mirandou, M. Fontana, B. Arcondo: X-ray analysis of  $\text{GeSeAg}$  glasses, *J. Non-Cryst. Solids* 273, 30 (2000).
13. Scher, H. Zallen, R. J. Chem.: Critical Density in Percolation Processes, *Phys.* 53, 3759 (1970) see also; R. Zallen, H. Scher: Percolation on a Continuum and the Localization-Delocalization Transition in Amorphous Semiconductors, *Phys. Rev. B* 4 4471 (1971).
14. B. Arcondo, M.A. Ureña, A. Piarristeguy, A. Pradel and M. Fontana: Homogeneous-inhomogeneous models of  $\text{Ag}_x(\text{Ge}_{0.25}\text{Se}_{0.75})_{(100-x)}$  bulk glasses, *Physica B* 389, 77 (2007).

15. A. Pradel, N. Kuwata and M. Ribes: Ion transport and structure in chalcogenide glasses, *J. Phys. Condens.Matter*, 15, S1561 (2003).

Figure captions.

Figure 1. Se rich corner of the Ag-Ge-Se equilibrium phase diagram. The shading zone corresponds to the liquid miscibility gap. The dashed lines show the composition of the analyzed samples.

Figure 2. Scanning electron micrographies of bulk glasses of composition  $\text{Ag}_{0.07}(\text{Ge}_x\text{Se}_{1-x})_{0.93}$  with  $x=0.25$  (A) and  $x=0.20$  (B) and  $\text{Ag}_{0.20}(\text{Ge}_x\text{Se}_{1-x})_{0.80}$  with  $x=0.25$  (C) and  $x=0.20$  (D).

Figure 3. Mössbauer spectra of powdered amorphous samples containing 0.5% Fe (90%  $^{57}\text{Fe}$ ) obtained in transmission geometry at room temperature. The spectra were fitted with two histogram distributions of quadrupole splitting  $\Delta$ . The velocity scale is referred to the Fe(Rh) source.

Figure 4. Mössbauer spectra of powdered  $\text{Fe}_{0.005}[\text{Ag}_{0.10}(\text{Ge}_{0.25}\text{Se}_{0.75})_{0.90}]_{0.995}$  amorphous sample obtained in transmission geometry at several temperatures. The spectra were fitted with two histogram distributions of quadrupole splitting  $\Delta$ . The velocity scale is referred to the Fe(Rh) source.

Figure 5. Magnetic moment density measurements of powdered glasses containing 0.5% Fe, from 5 to 300K, after a zero field cooling and a field cooling. The external field applied was 500Oe. The insets show the in phase component of the AC magnetic moment density of the corresponding sample.

Figure 6. Hysteresis cycles of  $\text{Fe}_{0.005}[\text{Ag}_{0.10}(\text{Ge}_{0.25}\text{Se}_{0.75})_{0.90}]_{0.995}$  glasses obtained at several temperatures. The fitting considering two components, a blocked one even up to room temperature that saturates at low field and a paramagnetic one that does not saturate even at the largest applied field, is also depicted.

Figure 1.

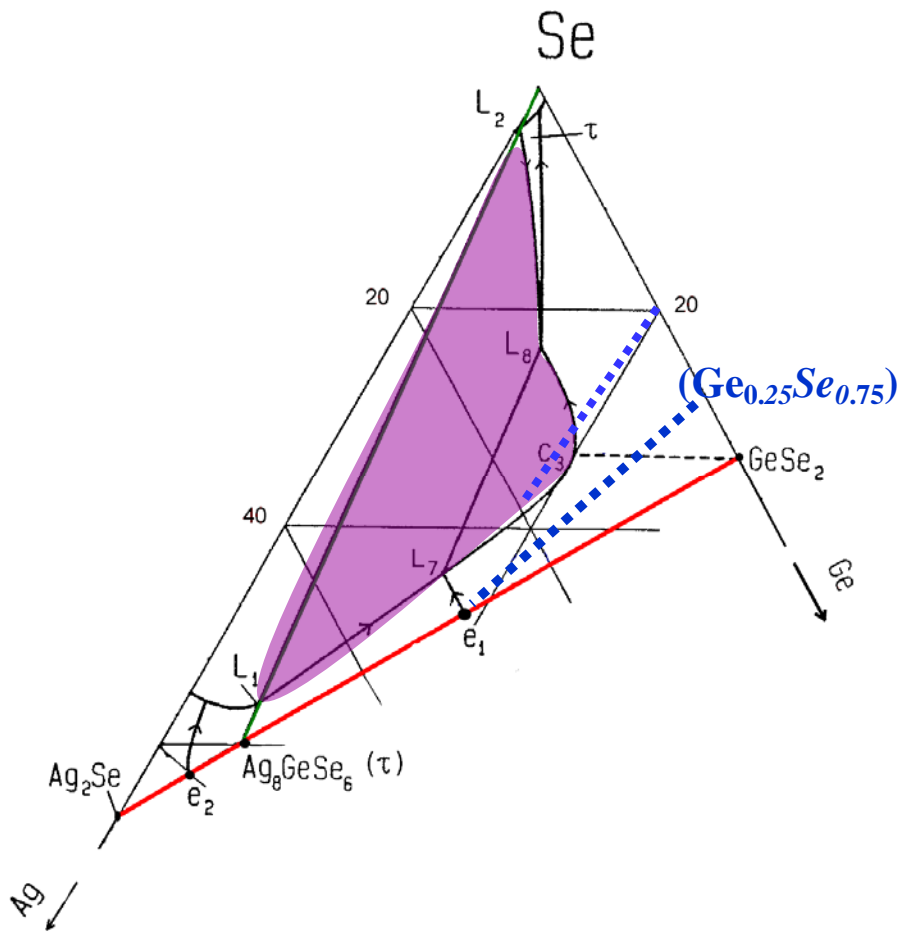


Figure 2.

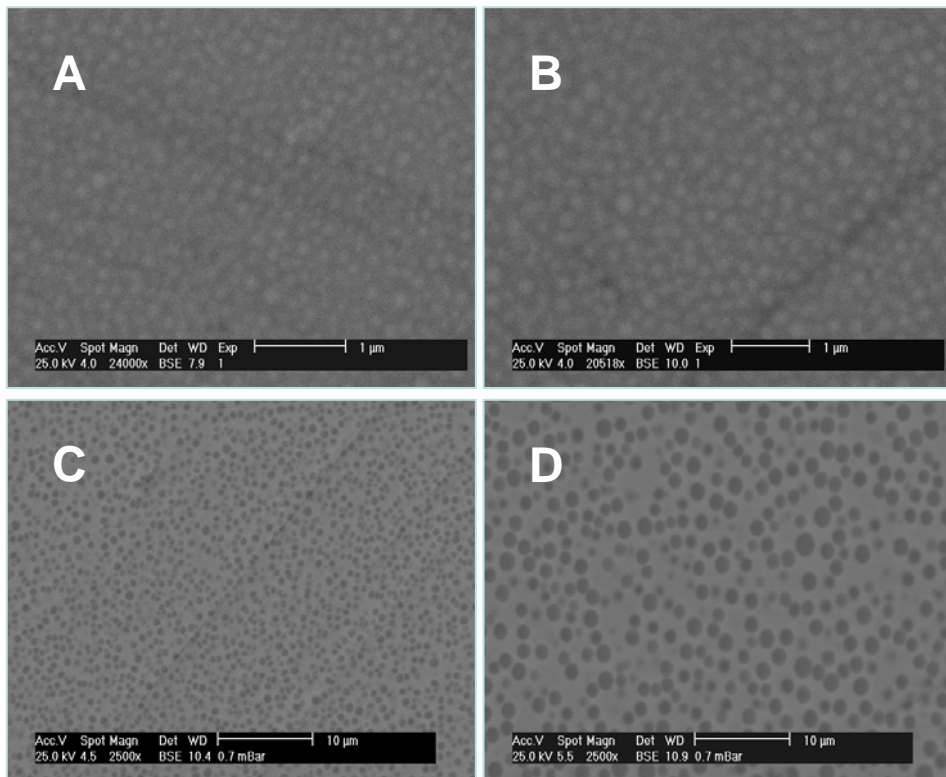


Figure 3.

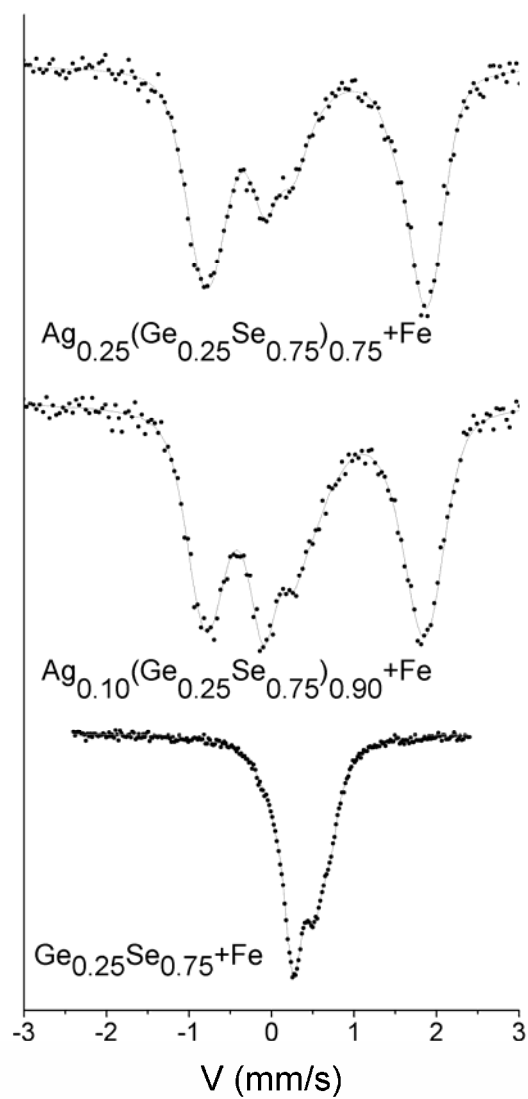


Figure 4.

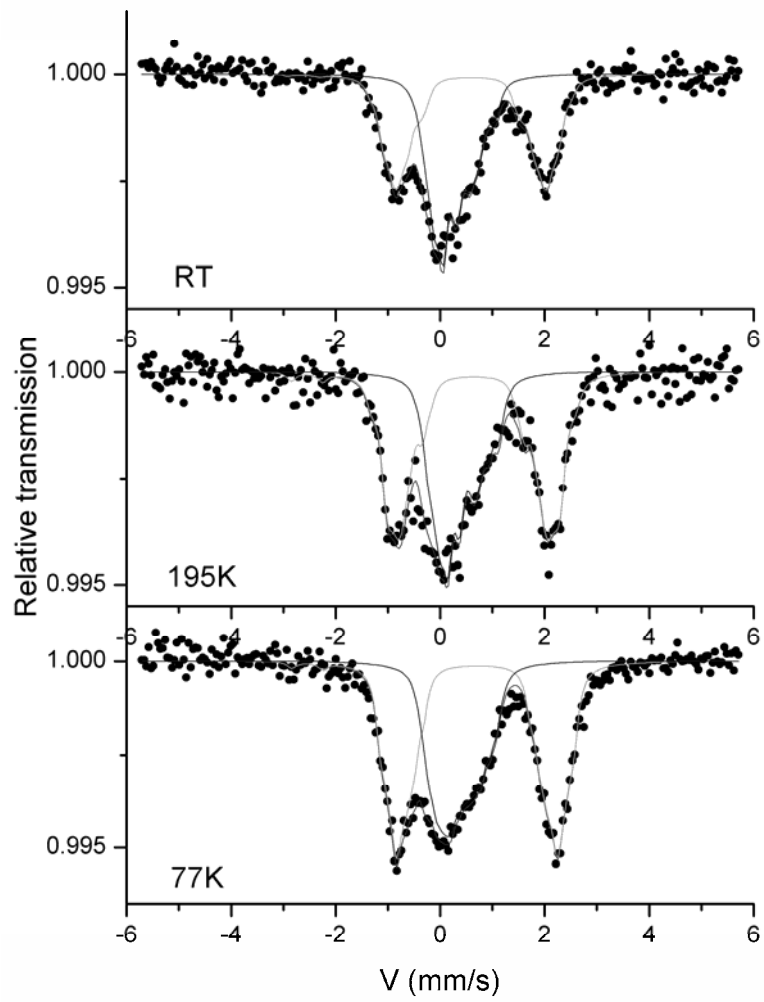


Figure 5.

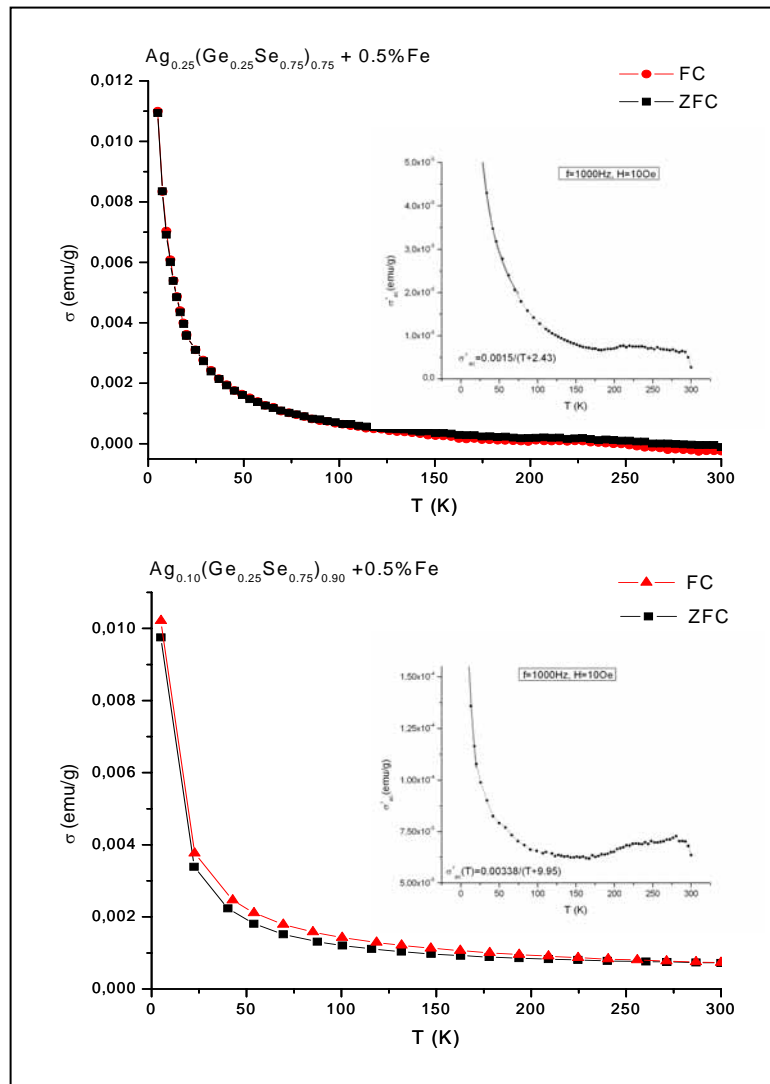


Figure 6.

